Proceedings of IDETC/CIE 2005
ASME 2005 International Design Engineering Technical Conferences & Computers and Information in Engineering Conference
September 24-28, 2005, Long Beach, California, USA

DETC2005-84272

ROTOR DROP TRANSIENT ANALYSIS OF AMB MACHINERY

R. G. Kirk
Mechanical Engineering Dept.
Virginia Tech
Blacksburg, VA 24061
gokirk@vt.edu

E. J. Gunter
RODYN Vibration Analysis, Inc.
Charlottesville, VA 22903
DrGunter@aol.com

W. J. Chen
Eigen Technologies, Inc.
Davidson, NC 28036
Dyrobes@apex.net

ABSTRACT

A major limitation of AMB supported machinery is their dependence on auxiliary or backup bearings in the event that the magnetic bearings lose power due to control system failure. These backup bearings should be designed to withstand the severe loads encountered after the AMB failure when the rotor drops onto them. This has prompted the development of general purpose finite element based, non-linear transient analysis programs capable of evaluating shock loading, blade loss and rotor drop phenomena experienced in rotors supported by AMBs. Previous testing and results have been made for a single AMB drop or both AMBs of a two bearing rotor. The current interest also includes the multiple AMB supported machinery systems, i.e., systems with more than two AMB or auxiliary bearings. This paper reviews the method of rotor drop analysis for AMB bearing systems. A commercially available program, DyRoBeS, is then applied to four different rotor designs to evaluate their rotor drop transient response. The total power loss rotor drop results of four different rotor systems will be discussed for assumed backup bearing conditions.

Keywords: transient, rotor drop, magnetic bearings, instability

INTRODUCTION

The rotor dynamic evaluation of turbomachinery plays an important role in the overall design process of all new rotating machines. The proper design of any AMB system requires the knowledge of all the dynamic loads that will ever be experienced by the rotor in its planned service. One of the major setbacks of the current high performance turbomachinery equipped with a AMB systems is their dependence on auxiliary or back-up bearings to support the rotor in case the AMB control system fails. These backup bearings have failed to withstand various dynamic loads in the event of AMB failure during both controlled test stand and field operating conditions. This motivated researchers to analytically predict the motion of the rotor and the impact loads subjected to the backup bearing following AMB failure. Ishii [1] applied transient response technique to simulate the rotor drop phenomena and predict the high instantaneous loads acting on the backup bearing. He performed the transient response analysis to simulate the rotor drop phenomenon for a two mass Jeffcott rotor system using the Runge-Kutta fourth order method. Gelin, Pugnet and Hagopian [2] studied the dynamic behavior of rotors on safety auxiliary bearings. Ishii and Kirk [3] described some analytical results on rotor drop and instantaneous loads on flexible backup bearings for a Jeffcott rotor model. Fumagalli, Feeny and Schweitzer [4] and Fumagalli, Varadi and Schweitzer [5] studied the dynamics and loads of a rigid rotor in a rigid bearing with clearance. Kirk and Ishii [6] extended their analytical capability by making improvements to their earlier model to more accurately simulate the actual flexible support systems. The vibrational behavior of a one ton compressor rotor being dropped into the auxiliary bearings after AMB failure has been reported by Schmied and Pradetto [7].

The need for a better understanding of the dynamics of the rotor drop phenomena, lead Kirk, et. al. [8] to set up a full scale test rig to evaluate various backup bearing configurations and to develop analytical tools to simulate complex turbomachinery supported by AMBs. Ramesh and Kirk [9] developed computational ability to perform finite element based steady state analysis of AMB turbomachinery and compared their results with experimental data. Raju, Ramesh, Swanson and Kirk [10] presented analytical results for finite element based rotor drop simulation and successfully compared them with experimental data. These simulations were done for cases with rigid backup bearings. The capability of the analytical tool was later enhanced by Raju [11], to take into account, various types of support flexibilities. Swanson, Raju and Kirk [12] and Kirk, Raju and Ramesh [13] presented some of the results obtained using that computer program. The current industrial design interests are for the drop of AMB supported rotor systems, including the controller degrees of freedom and also including two or more non linear backup bearings. Modern design analysis also requires a more

advanced pre and post processor for initial model generation and presentation of the results. The results presented in this paper to evaluate the stability of multiple bearing rotor drop, were generated using a commercial computer program, DyRoBeS [14-16].

.

Finite Element Modeling of Rotor-Bearing Systems

The process of theoretically modeling any physical system for numerical simulation purposes consists of isolating the parameters influencing the dynamic nature of that system and developing the mathematical equations which represent the actual system as closely as possible. These equations are then solved using optimum numerical methods to obtain the desired results for predicting the actual system dynamics. The current process of modeling turbomachinery supported by AMBs requires the knowledge of finite element discretization of rotor-bearing systems. In addition, the various numerical methods capable of efficiently performing transient analysis using the dynamic equilibrium equations of this particular system should be considered to provide the best solution technique. The influence and relationships of various parameters are described in more detail in the following discussion.

The dynamic equilibrium equation for a rotor-bearing system can be represented in matrix form as follows when the speed of operation is constant:

$$\mathbf{M}\ddot{\mathbf{q}} + \mathbf{C}\dot{\mathbf{q}} + \mathbf{K}\mathbf{q} = \mathbf{F} \qquad (1)$$

where $\boldsymbol{M}$, $\boldsymbol{C}$, and $\boldsymbol{K}$ are the mass, damping and stiffness matrices obtained from finite element discretization. The state vectors $\ddot{\boldsymbol{q}}$, $\dot{\boldsymbol{q}}$ and $\boldsymbol{q}$ are the acceleration, velocity and displacement vectors of the system. $\boldsymbol{F}$ is the external force vector which propels the system. The shaft also known as rotor element is modeled as a beam element. The disks and turbine blades are modeled as discrete external mass elements having inertia and mass properties. Bearings, seals, etc. are modeled as discrete elements having stiffness and damping. The Z-axis of the reference frame coincides with the centerline of the rotor element. The displacement vector for the global finite element matrices can be written as :

$$\mathbf{q} = \left\{x_1, y_1, \theta_{x1}, \theta_{y1}, ..., x_n, y_n, \theta_{xn}, \theta_{yn}\right\}^{\mathrm{T}} \qquad (2)$$

where 'n' is the number of nodes in the global finite element model.

The acceleration vector $\ddot{\mathbf{q}}$ and velocity vector $\dot{\mathbf{q}}$ are in the same order as the displacement vector. The external force vector $\boldsymbol{F}$ is also in the same order. Forces are applied along the translational degrees of freedom at each node and moments are applied about the axis in which the corresponding degree of freedom rotates.

Simulation of rotating machinery requires the knowledge of all the static and dynamic forces or loads acting on the system. Loads due to gravity, bearing misalignment, gear forces or steady maneuvers, do not change with time and are known as static loads. Loads that change with time such as imbalance, blade loss, and loading from aerodynamic effects or compressor surge are known as dynamic loads. Non-linear transient analysis can be performed with the finite element model of rotor-bearing systems using a direct integration method by taking into effect the influence of some of the above mentioned static and dynamic loads. In the case of rotating machinery supported on magnetic bearings, the number of effective components of the external force vector differ depending upon whether the bearings are active or not. The axial movement of the nodes in the rotor model and the presence of the thrust magnetic bearing are ignored in this discussion.

Auxiliary Bearing with Multiple Layers of Contact Stiffness

A general backup bearing and support system could be represented as shown in Fig 1. The contact stiffness can be treated as varying stiffness and damping parameters, as a function of deformation of the auxiliary bearing and the associated housing stiffness and damping.

The evaluation of the auxiliary bearing can be treated in DyRoBeS by a multiple segment description of the auxiliary bearing stiffness and damping. The initial non-contact stiffness gap is followed by one or more additional rings of stiffness and damping. This option gives the user the ability to specify the auxiliary bearing gap, contact stiffness which is the soft mounting stiffness and the limit stiffness after a given deformation. This is the option that has been utilized for the results presented in this paper.

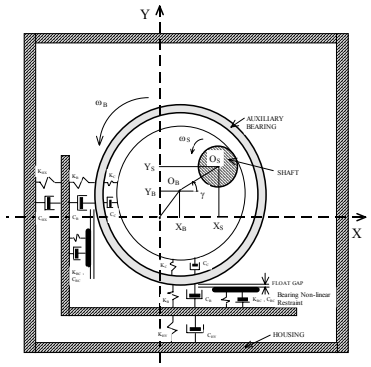

Fig. 1: Cross-section of any typical AMB at the back-up bearing.

SPECIAL CONCERNS FOR MULTIPLE BEARING MACHINERY ANALYSIS

A continuous rotor system with multiple bearings is statically in-determinant and must be solved with the foundation support system stiffness characteristics. The AMB controller bias force produces a very stiff bearing static stiffness to center the rotor to the desired location within the clearance space. The loading will change as a function of the support stiffness. The more flexible the coupling(s) of multi-body systems, the less important will be this effect for two bearing components.

The actual bias loading on the non-drop AMB's during the initial rotor drop is also not easily determined. The non drop location bias loads are therefore not considered to change during the drop and resulting transient motion. The transient short duration impact forces that are generated are reacted by the dynamic stiffness and damping of any of the other active bearings still under control. Multiple bearing machines will likely have one controller for each set of two active bearings. A typical configuration could be a four bearing machine having

a driver and compressor or pump for example. A double extended motor could be used to drive compressors or pumps on either end resulting in a six bearing support system and six or more backup bearings. It is possible to have four auxiliary bearings on a standard two bearing compressor or pump to better protect the stator if the shafting is very flexible. The rotor dynamics of multiple bearing, multiple body rotor systems with rigid or near rigid couplings is not documented in great detail for high speed machinery. Turbo-generator units with fluid-film bearings are the most likely machinery to have been solid coupled and documented with regard to loading and unloading of bearings due to alignment problems. The analysis of solid coupled multi-bearing machines is complicated by the number of modes that must be considered. For example the typical third mode or first free-free forward mode of a two-bearing machine becomes the seventh or higher forward mode for a six bearing rotor system that has essentially three bodies connected by two rigid couplings(see Example 4 in the following discussion of this paper).

The DyRoBeS computer program can evaluate a system with from one to 100 AMB supported bearings and 100 auxiliary bearings. Any number of AMB drop locations, from one to **100,** can be evaluated. The rotor model may contain up to 500 rotor stations. The computation time for a typical constant speed drop is 3 minutes or less using a 1.7 GHz Pentium IV processor. The evaluation of a changing speed or time dependent non-linear forcing will increase the execution time to several hours. The integration process can use either a Runge Kutta, a Newmark-β method or a Wilson-θ calculation which can include numerical damping for higher modes **(**see Craig [17], Bathe[18])**.** Due to the similarity of the Newmark-β and the Wilson-θ method, they can be implemented in a single computer subroutine or function.

SPECIAL CONSIDERATION FOR STARTUP AND SHUTDOWN SIMULATION

There are two types of transient analysis. One is the rotor system with a constant rotational speed, and the other one is with a variable rotational speed. For a constant rotational speed, the transient analysis is used to determine the steady state response for the non-linear systems or the linear/nonlinear systems subject to sudden excitations. In many applications, there are needs to study the rotor motion during startup, shutdown, going through critical speeds, or rotor drop when the magnetic bearings failure occurred. In these situations, the angular velocity (spin speed) is no longer a constant and is a function of time. The governing equations of motion for a constant rotational speed have been presented before, the governing equations of motion for a variable rotational speed system are:

$$\begin{aligned}\mathbf{M}\ddot{\mathbf{q}}(t)+\left[\mathbf{C}+\dot{\varphi}\mathbf{G}\right]\dot{\mathbf{q}}(t)+\left[\mathbf{K}+\ddot{\varphi}\mathbf{G}\right]\mathbf{q}(t)\\ =\dot{\varphi}^2\mathbf{Q}_1(\varphi)+\ddot{\varphi}\mathbf{Q}_2(\varphi)+\mathbf{Q}_3(\dot{\mathbf{q}},\mathbf{q},\varphi,\dot{\varphi},\ddot{\varphi},t)\end{aligned} \tag{3}$$

Two more terms introduced in the governing equations due to the speed variation are: circulatory matrix $\dot{\varphi}\mathbf{G}$ and forcing function $\ddot{\varphi}\mathbf{Q}_2$. At any time instant, the angular velocity $\dot{\varphi}=\Omega$. All the linearized damping and stiffness terms are in the damping and stiffness matrices and all the other interconnection nonlinear forces are included in $\boldsymbol{Q}_3$. $\boldsymbol{Q}_1$ and $\boldsymbol{Q}_2$ are functions of $(\varphi,\dot{\varphi})$ and $(\varphi,\ddot{\varphi})$, respectively. For mass unbalance, $\boldsymbol{Q}_1$ and $\boldsymbol{Q}_2$ at station "*i*" can obtained from the following expression:

$$\begin{Bmatrix}F_{u,x}\\F_{u,y}\\M_{u,x}\\M_{u,y}\end{Bmatrix}=\dot{\varphi}^2\begin{Bmatrix}me\cos\varphi\\me\sin\varphi\\0\\0\end{Bmatrix}+\ddot{\varphi}\begin{Bmatrix}me\sin\phi\\-me\cos\phi\\0\\0\end{Bmatrix} \tag{4}$$

For a system with a constant rotational speed ($\dot{\varphi}=\Omega,\ddot{\varphi}=0$) and for a system with a variable rotational speed ($\dot{\varphi}=\Omega,\ddot{\varphi}\neq 0$), the transient response can to be obtained by direct numerical integration algorithms in the physical coordinates. For simplicity of notion, the equations of motion, equation (3) can be rewritten as:

$$\mathbf{M}\ddot{\mathbf{q}}(t)+\overline{\mathbf{C}}\,\dot{\mathbf{q}}(t)+\overline{\mathbf{K}}\,\mathbf{q}(t)=\mathbf{Q} \tag{5}$$

EXAMPLE ROTOR DROP RESULTS

The results presented in this paper have considered the initial position of the rotor to be at the center of the bearings at the drop time with the gravity load acting. All of the AMB locations are assumed to be inactive and the only bearings in the system are the auxiliary bearings with the clearance gap. The rotor imbalance is also applied at this instant in time. This is considered to be a worst case condition for evaluation of the transient drop dynamics. The computation of the drop transient using the non linear AMB capability of DyRoBeS for a motor compressor system is currently being evaluated but none of those results can be included in this discussion. The following rotor drop examples will first consider a high speed turbo test rotor for assumed conditions at the auxiliary bearings, then the results of a former test rotor from Virginia Tech with 3 major disk locations, then with 5 disk locations to lower the free-free mode frequency, and finally a six bearing compressor-motor-compressor train evaluation.

Example 1: A turbo test rotor configuration

The turbo test rotor as modeled has a length of 0.851 m, mass of 25.963 kg and can operate at speeds to 30,000 rpm and higher. The diameter of the shaft at the AMB is 0.063 m and at the auxiliary bearing it is 0.0396 m. The rotor is shown in Fig 2 with the two bearing locations showing at the auxiliary bearing locations. The undamped critical speed map is given in Fig 3 and the free-free mode is observed to be above 40,000 rpm with the lower two modes being clearly rigid rotor modes for bearing stiffness levels below 10E8 N/m. The free-free mode shape is shown in Fig 4 to be 43152 cpm or 719 Hz. The constrained static deflection is presented in Fig 5, with a max deflection of 2.57 μm, again indicating a rigid rotor design. The midspan imbalance is 5E-5 kgm for the following drop case results.

The results of the rotor drop at 30000 rpm and decel to 10000 rpm is given in Fig 6, where the 3D orbits show a well

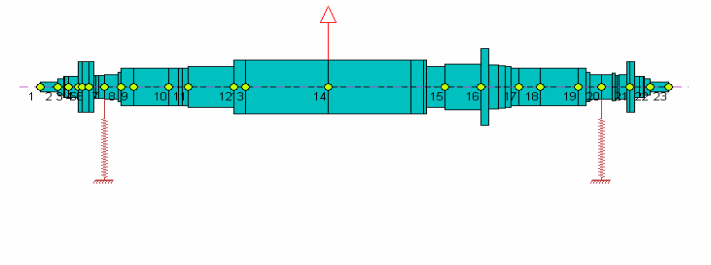

Fig 2 Turbo Test Rotor

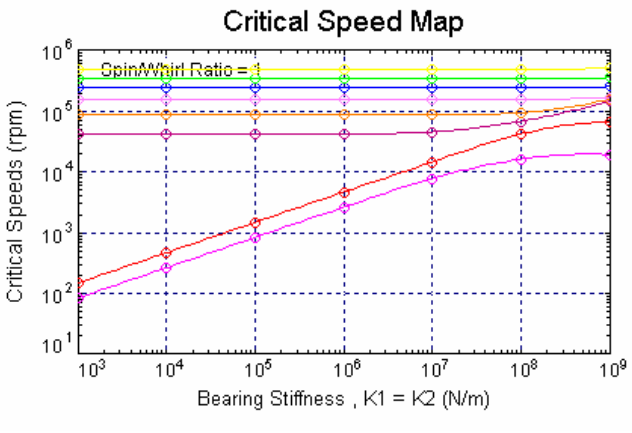

Fig 3 Turbo Test Rotor Undamped Critical Speed Map

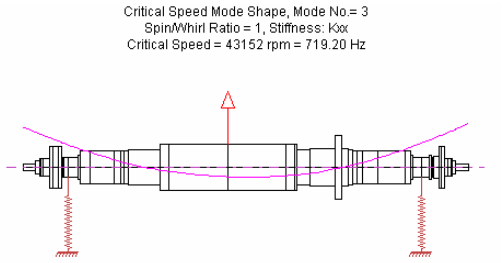

Fig 4 Test Rotor Free-Free Mode

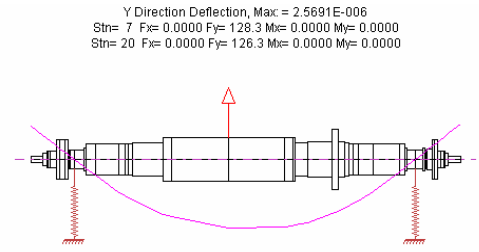

Fig 5 Test Rotor Static Deflection

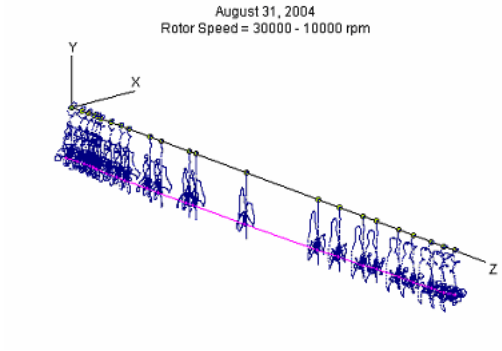

Fig 6 Test Rotor 3D Station Orbits for Drop at N = 30 000 and decel to 10 000 rpm

behaved drop, with only a small side movement. This is confirmed by the time traces of the bearing force and response for the first bearing location, station 7, given in Figs 7 and 8. The orbit x-y motion at station 7 and 20, bearing 1 and 2 respectively, show an initial bounce then rapid decay to a small motion(see Figs 9-10). A drop at below the free-free mode is considered as a good design for AMB support rotors.

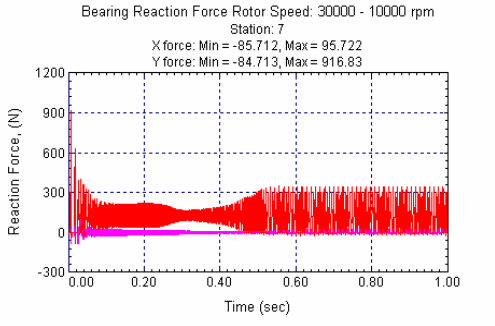

Fig 7 Sta 7 Brg 1 Force vs time, 30k to 10k rpm

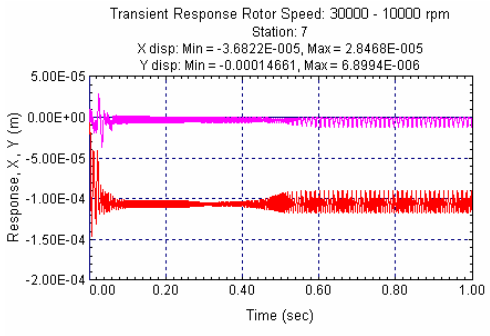

Fig 8 Sta 7 Brg 1 Resp vs time, 30k to 10k rpm

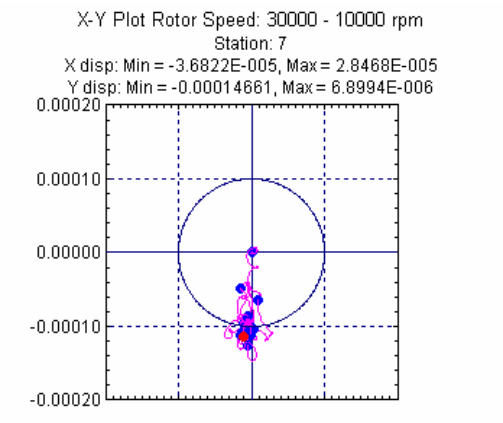

Fig 9 Brg 1 Orbit for Drop, 30k to 10k rpm

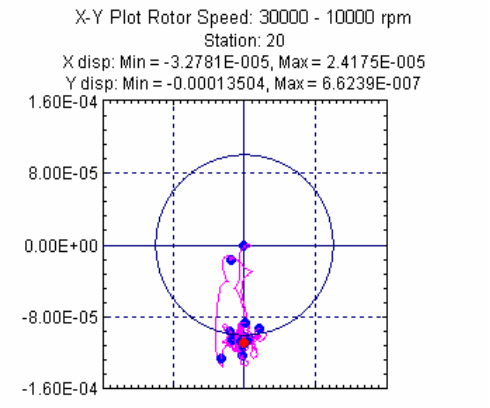

Fig 10 Brg 2 Orbit for Drop, 30k to 10k rpm

With the rotor speed increased to 50000 rpm, a 0.04 second drop at constant speed is shown in Fig 11. This shows increased activity at the bearing locations. The orbit trace and force transmitted at bearing 1 and 2 are presented in Figs 12-13 and 14-15. It clear in these force plots that the rotor rebounds from the bearing after the initial contact, and the forces are slightly higher than for the 40000 rpm drop. For the constant speed, the FFT spectrum is possible and it clearly shows energy at running speed but also at the free-free mode frequency. The largest spikes are for frequencies below 5000 cpm as shown in Figs 16-17.

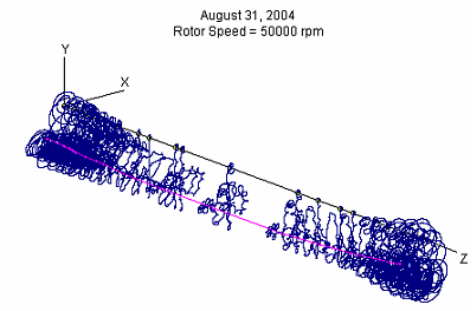

Fig 11 Test Rotor 3D Station Orbits for Drop at N = 50 000

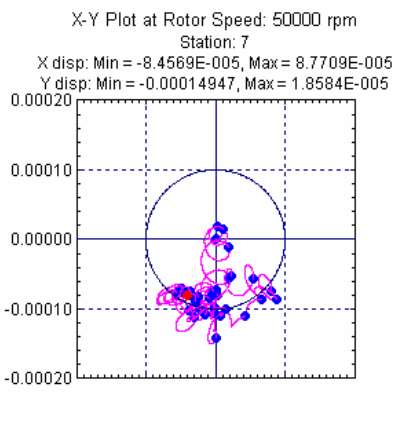

Fig 12 Brg 1 Orbit for Drop, 50k rpm

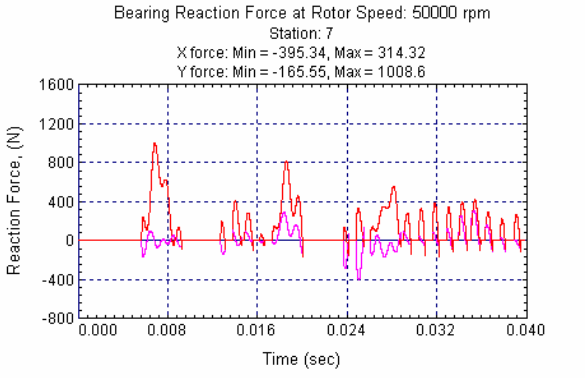

Fig 13 Brg 1 Force for Drop, 50k rpm

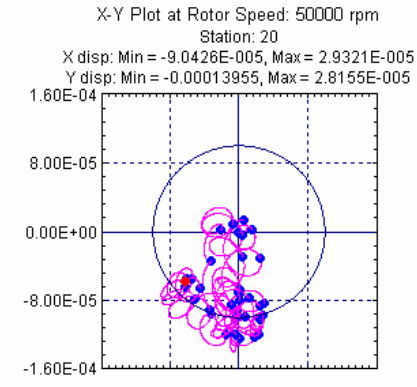

Fig 14 Brg 2 Orbit for Drop, 50k rpm

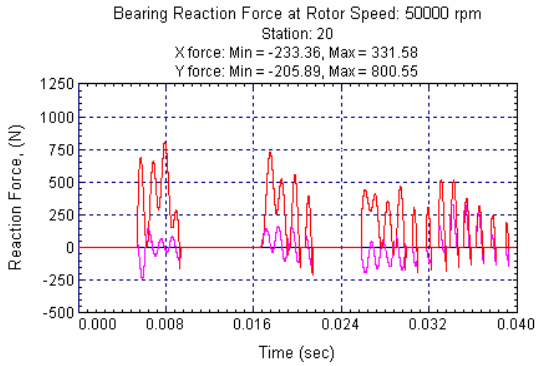

Fig 15 Brg 2 Force for Drop, 50k rpm

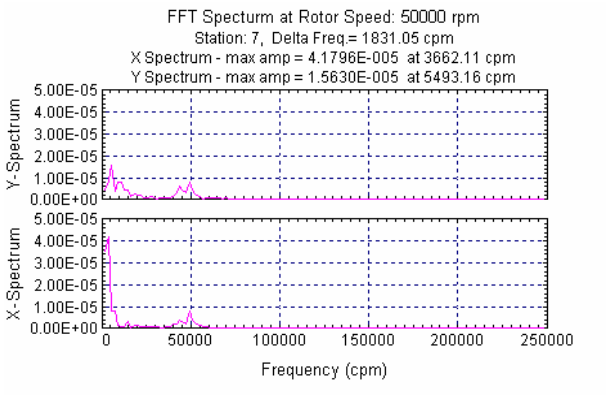

Fig 16 Brg 1 FFT for Drop, 50k rpm

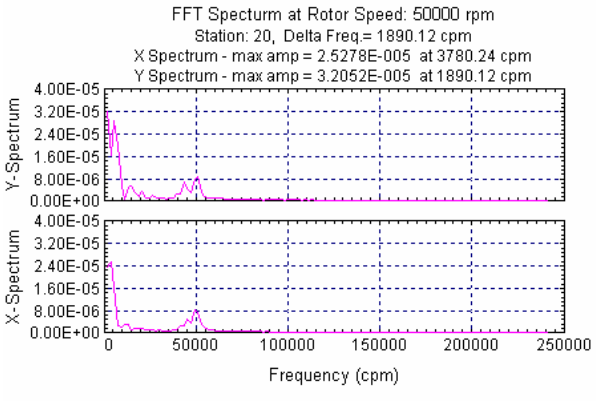

Fig 17 Brg 2 FFT for Drop, 50k rpm

The result of a drop at 50000 and decel to 40000 rpm, during a one second time period, is given in Figs 18 – 20. The 3D rotor response clearly shows large whirling and the orbit plots for bearing one shows the rotor motion taking the entire clearance gap of the auxiliary bearing. The bearing reaction and response versus time clearly indicate the danger of coming down through the free-free, even at the rate of 10000 rpm per second. The peak force is in excess of 5000 N, while the static load is only 128 N and numerous peaks of 2000 N are observed for bearing one. The vertical motion goes from -172 µm to 121 µm. The gap clearance is only 100 µm and the soft spring retainer goes very stiff at 170 µm. A slow unloaded decel through this speed range would not be tolerated by the retainer bearings most likely.

Example 2: A 3 disk solid rotor.

Limited testing of soft mount solid bushing were conducted at Virginia Tech in the mid 1990's using a rotor similar to that shown in Fig 21. The free-free mode for this rotor is at 37000 cpm (615 Hz), while the actual rotor test speed was only 8000 rpm (133 Hz). The critical speed is similar to the turbo test rotor of example 1, in that the desirable operation speed range is below the free-free mode. This rotor has a length of 62.84 in (1.6 m) and a mass of 310 lb (141 kg). The auxiliary bearing diameter is 3.527 in (89.6µm). The results shown in Figs 22 – 26 show a well behaved drop and rapid reduction to a small response and force level. The rotor has a single 1.0 oz-in imbalance at midspan for this drop.

This simulation gives added confidence that drops below the free-free mode of a two bearing rotor system has a low risk for system damage. The assumption of proper bearing operation for the duration is assumed in these results. If a higher friction is in effect or a larger rotor imbalance, the results would show higher force levels without doubt, but safe operation would be expected for normal operating conditions. The actual test results agree with these conclusions.

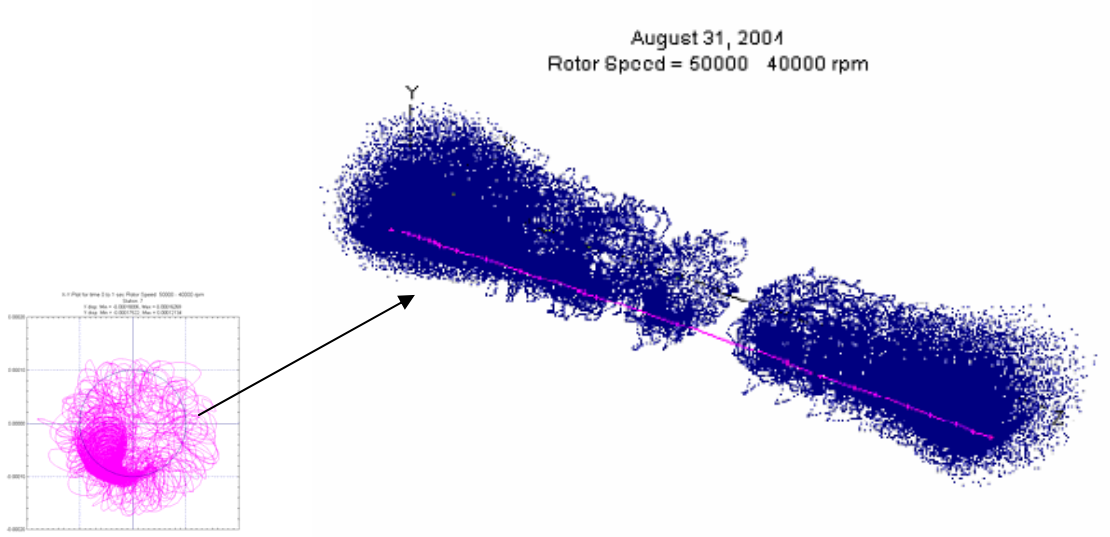

Fig 18 Test Rotor 3D Station Orbits for Drop at N = 50 000 and Decel to 40 000 rpm

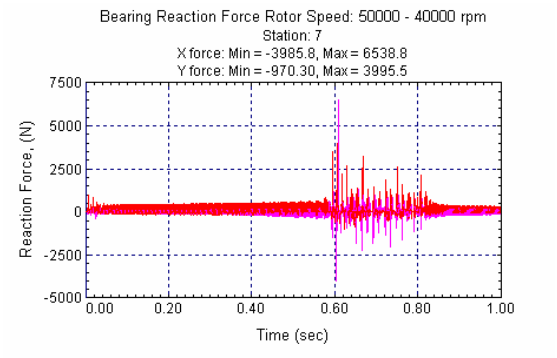

Fig 19 Brg 1 Reaction for Drop, 50k-40k rpm

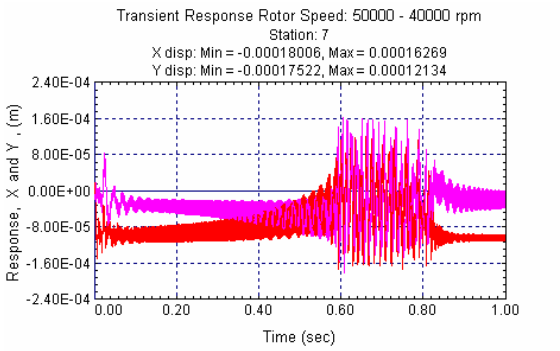

Fig 20 Brg 1 Response for Drop, 50k-40k rpm

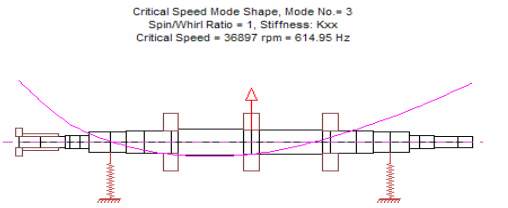

Fig 21 3 Disk VT Rotor, free-free mode shape

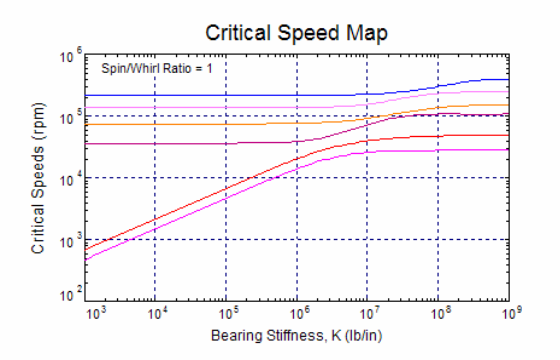

Fig 22 3 Disk VT Rotor, Critical Speed Map

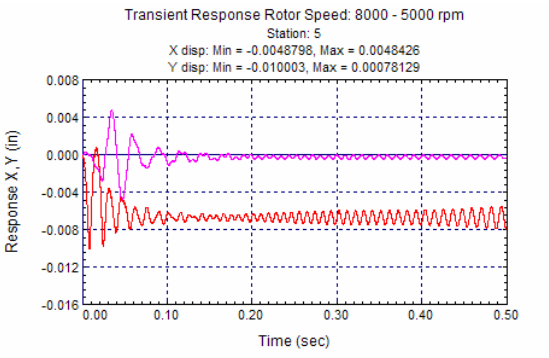

Fig 23 3 Disk VT, Brg 1Response 8k -5k rpm

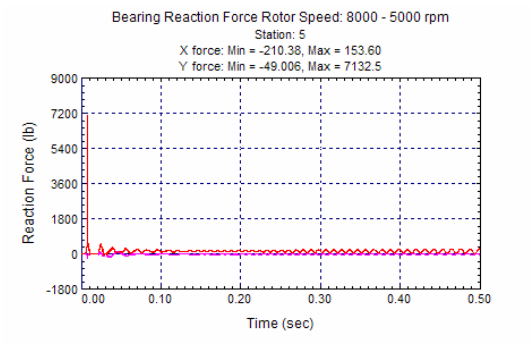

Fig 24 3 Disk VT, Brg 1 Force for 8k-5k rpm

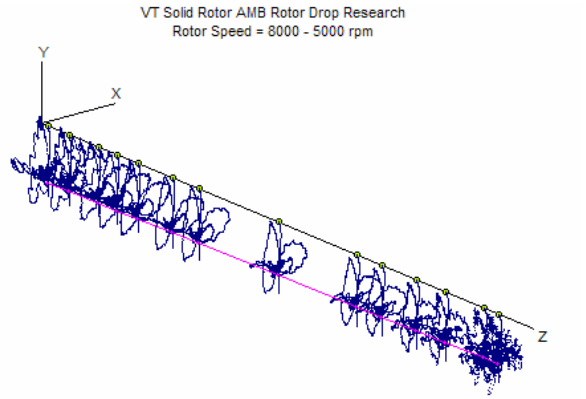

Fig 25 3 Disk VT, Drop 8k -5k rpm

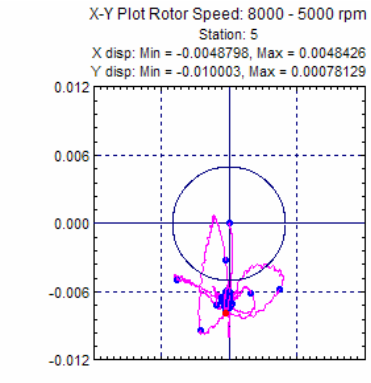

Fig 26 3 Disk VT, Brg 1 Orbit for 8k-5k rpm

Example 3: A 5 disk solid rotor

The rotor used in Example 3 was initially going to run with added disks at the outboard locations, making it a 5 disk rotor. The configuration is shown in Fig 27 and the critical speed map is given in Fig 28. The free-free mode is clearly lower, down to about 7400 cpm (123 Hz) as shown in Fig 29. The rotor has a mass of 540 lb (245 kg). The rotor has a 1.0 oz-in imbalance at midspan and 0.5 oz-in at 180 degrees at each outboard disk location for this drop. A snap decel gave reasonable results, but the 1 second decel from 9000 to 6000 rpm (see Fig 30) allowed a great increase in levels at 0.7 seconds into the decel, the levels were excessive and the computation stopped (see Figs 31 – 33). The build up in amplitude shows forces at near 1000 lb (4448 N) and a rapidly increasing spiral of the rotor response at the bearing and much greater at the overhang locations.

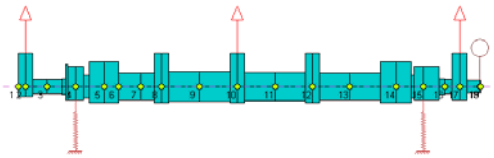

Fig 27 5 Disk VT Rotor model

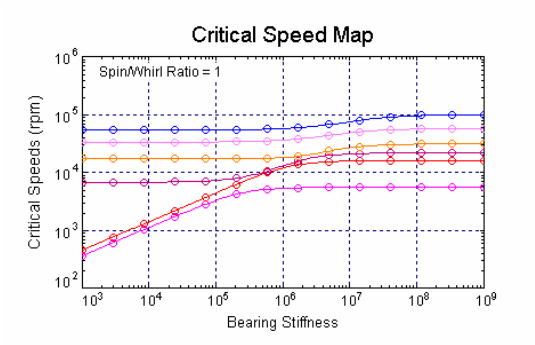

Fig 28 5 Disk VT Rotor, Critical Speed Map

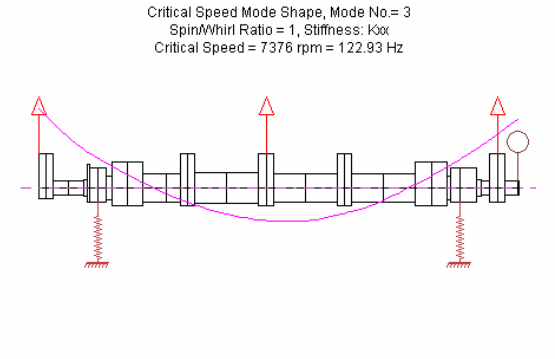

Fig 29 5 Disk VT Rotor, free-free mode shape

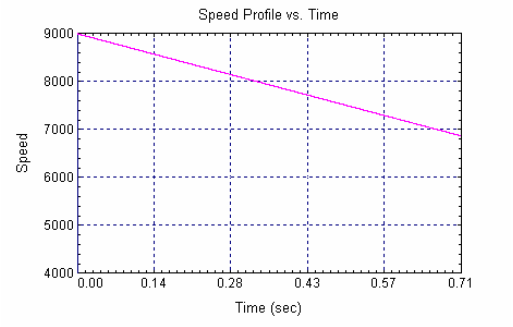

Fig 30 5 Disk VT Rotor, Speed versus time

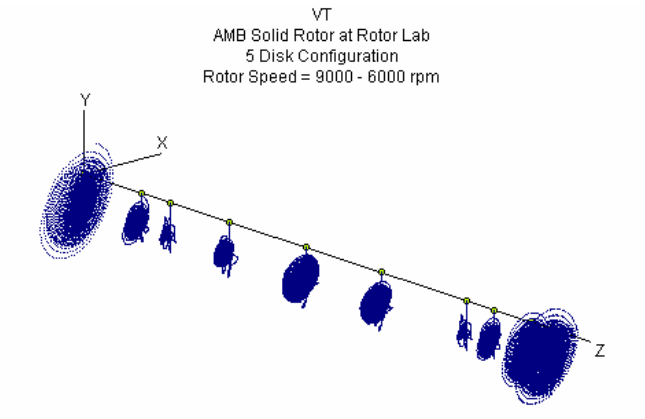

Fig 31 5 Disk VT Rotor Transient for decel from 9000 to 6800 rpm

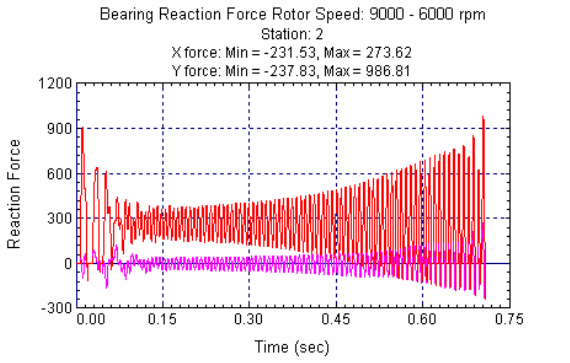

Fig 32 5 Disk VT Rotor, brg 1 Reaction Force

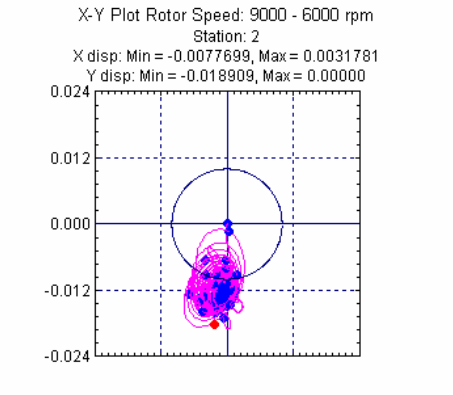

Fig 33 5 Disk VT Rotor, Brg 1 Orbit

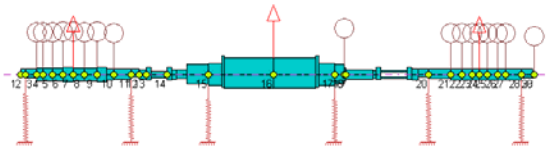

Fig 34 6 Brg 3 Rotor model for drop simulation

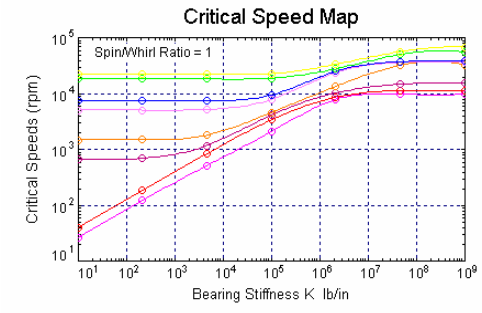

Fig 35 Ncr Map

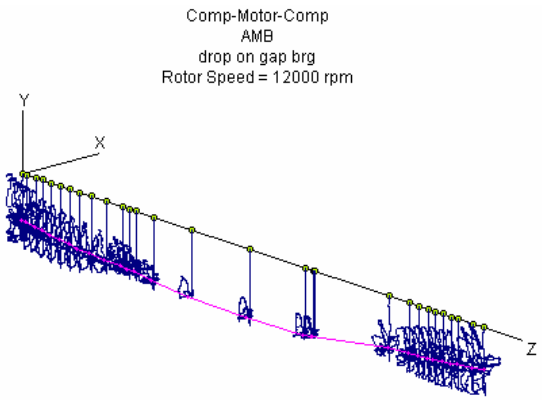

Fig 36 Transient Response for a drop at 12000 rpm

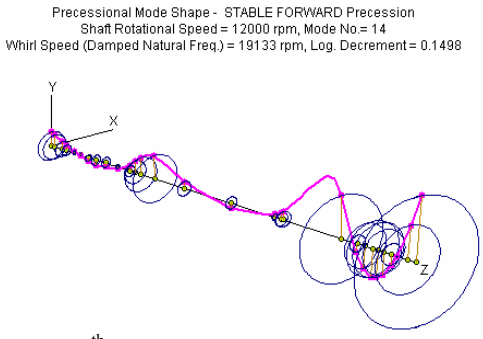

Fig 37 14th Damped Mode when N = 12000 rpm

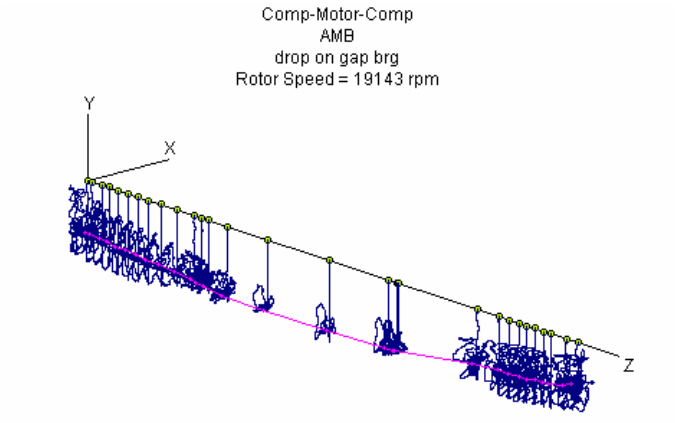

Fig 38 Transient Response for a drop at 19143 rpm

Example 4: A 3 body 6 bearing industrial configuration

The compressor-motor-compressor configuration shown in Fig 34 was evaluated for rotor drop several years ago using the Virginia Tech FEA transient analysis and found to be marginally acceptable. The results of a recent limited evaluation using DyRoBeS is presented as the final example for this discussion. The critical speed map is given in Fig 35 but the first free-free mode is not likely the mode of concern, rather the 7th forward circular mode of this plot. The lower modes are partial rigid body modes and are somewhat damped by the multiple bearing locations. The initial results found that the compressors had increased activity while the heavier motor had less response. This solid coupled train of equipment has a total mass of 2893 lb (1312.kg) and a total length of 16.5 ft (5 m). The system is supported on six AMBs and has six auxiliary bearings. The rotor has a single 1.0 oz-in imbalance at the motor and 0.5 oz-in at 180 degrees at the midspan of each compressor. The drop transient response at 12000 rpm shown in Fig 36, is similar to the former study drop result, with much greater activity at the compressors. The 14th mode (7th forward mode in fact) is shown in Fig 37, where all 3 bodies are in a connected (constrained) free-free mode shape. The drop at a speed very close to this mode 14 frequency does not give greatly increased levels of amplitude (see Fig 38). A slow decel through this speed region may in fact give a more violent response, but the present results do not indicate this to be true in fact. The actual operating speed was much lower and this is hence only of academic interest at this point. More

detailed evaluations of such systems will be made in future studies of multi-bearing machinery.

SUMMARY

The results of this paper confirm the large amplitudes of response and force to the auxiliary bearings for a drop near a single rotor free-free natural frequency. The rotor drop and decel studies using DyRoBeS have predicted an even higher level of response for the moderate decel rates through these critical speeds. The results from the analysis are easily reduced in graphic form for presentation at design review discussions. The program is capable of greater detail of the rotor system and the AMB bearing than previous specialized computer programs [19].

AKNOWLEDGMENTS

This work was sponsored by the Virginia Tech Rotor Dynamics Laboratory Industry Affiliates Group.

REFERENCES

1. Ishii, T., 1990, “Transient Response Technique Applied to Active Magnetic Bearing Machinery During Rotor Drop”, Master of Science Thesis, Mechanical Engineering Department, Virginia Tech, Virginia
2. Gelin, A., Pugnet, J.M., and Hagopian, J.D., 1990, “Dynamic Behavior of Flexible Rotors with Active Magnetic Bearings on Safety Auxiliary Bearings”, Proceedings of 3rd International Conference on Rotordynamics, Lyon, France, pp. 503-508.
3. Ishii, T., and Kirk, R.G., 1991, “Transient Response Technique Applied to Active Magnetic Bearing Machinery During Rotor Drop”, ASME Conference Proceedings, DE-Vol. 35, pp. 191-200.
4. Fumagalli, M., Feeny, B., and Schweitzer, G., 1992, “Dynamics of Rigid Rotors in Retainer Bearings”, Proceedings of The Third International Symposium on Magnetic Bearings, Alexandria VA, July, pp. 157-168.
5. Fumagalli, M., Varadi, P., and Schweitzer, G., 1994, “Impact Dynamics of High Speed Rotors in Retainer Bearings and Measurement Concept”, Proceedings of Fourth International Symposium on Magnetic Bearings, August 1994, Zurich, pp. 239-244.
6. Kirk, R.G., and Ishii, T., 1993, “Transient Rotor Drop Analysis of Rotors following Magnetic Bearing Power Outage”, Proceedings of MAG ‘93, pp. 53-61.
7. Schmied, J., Pradetto, J.C., 1992, “Behavior of a One Ton Rotor Being Dropped into Auxiliary Bearings”, Proceedings of The Third International Symposium on Magnetic Bearings, Alexandria VA, July, pp. 145-156.
8. Kirk, R.G. Swanson, E.E. Karavana, F.H. Wang, X. Virginia Polytechnic Inst., "Rotor Drop Test Stand for AMB Rotating Machinery, Part I: Description of Test Stand and Initial Results," Proceedings of The Fourth International Symposium on Magnetic Bearings at The International Center for Magnetic Bearings, ETH Zurich, Switzerland, August 23-26, 1994, pp. 207-212.
9. Ramesh, K., and Kirk, R.G., 1992, “Subharmonic Resonance Stability Prediction for Turbomachinery with Active Magnetic Bearings”, Proceedings of the Third International Symposium on Magnetic Bearings, Alexandria, VA, pp. 113-122, 1992.
10. Raju, K.V.S., Ramesh, K., Swanson, E.E. and Kirk, R.G., 1995, “Simulation of AMB Turbomachinery for Transient Loading Conditions”, Proceedings of MAG ’95, Alexandria, VA, pp. 227-235.
11. Raju, K., May 1996, “Finite-Element Based Non-linear Transient Response Analysis of AMB Turbomachinery”, Master of Science Thesis, Mechanical Engineering Department, Virginia Tech, Virginia.
12. Swanson, E., Raju, K. and Kirk, R., 1996, “Test Results and Numerical Simulation of AMB Rotor Drop”, IMechE 1996, England, C500/074, pp. 119.
13. Kirk, R., Raju, K. and Ramesh, K., May 1996, “Evaluation of AMB Rotor Drop Stability”, The Eighth Workshop on Rotordynamic Instability Problems in High Performance Turbomachinery, Turbomachinery Laboratory, Texas A & M University, Texas.
14. DyRoBeS, version 9.1, Eigen Technologies Inc., 2004.
15. Chen, W. J., 1998, “A Note on Computational Rotor Dynamics,” ASME Journal of Vibration and Acoustics, Vol. 120, pp. 228-233.
16. Chen, W. J. and H. M. Chen, 1999, " Rotor Transient Response with Fault Tolerant Magnetic Bearings," Proceedings of Asia-Pacific Vibration Conference, Nanyang Technological University, pp. 53-58.
17. Craig, R. R., 1981, "Structural Dynamics: an Introduction to Computer Methods" John Wiley & Sons, Inc., pp. 452-455.
18. Bathe, K. J., 1995, "Finite Element Procedures", Prentice-Hall, Inc.
19. Kirk, R. G. "Evaluation of AMB Turbomachinery Auxiliary Bearings," *ASME Trans*, *Journal of Vibration and Acoustics* Vol. 121 , 2, 1999, pp. 156-161 .